Proceedings of the 28th IEEE
EMBS Annual International Conference
New York City, USA, Aug 30-Sept 3, 2006

Inter-Modality Variation in Gross Tumor Volume Delineation in ^{18}FDG-PET Guided IMRT Treatment Planning for Lung Cancer

Yulin Song, *Member*, *IEEE*, Maria Chan, Chandra Burman, and Donald Cann

***Abstract*: Rapid advances in ^{18}FDG-PET/CT technology and novel co-registration algorithms have created a strong interest in ^{18}FDG-PET/CT's application in intensity modulated radiation therapy (IMRT) and image-guided radiation therapy (IGRT). Accurate target volume delineation, particularly identification of pathologically positive lymph nodes, could translate into favorable treatment outcome. However, gross tumor volume (GTV) delineation on both CT and ^{18}FDG-PET is very sensitive to observer variation. The objectives of the study were to investigate the inter-modality variation in gross tumor volume delineation defined by two imaging modalities for lung cancer: CT and ^{18}FDG-PET/CT and its dosimetric implications in intensity modulated radiation therapy (IMRT).**

I. INTRODUCTION

According to the latest statistics, approximately three million new lung cancer cases are diagnosed each year world wide. About 170,000 cases will be in the United States this year and more than 150,000 patients will die of this disease. Lung cancer has become the most common cause of death from cancer in both men and women in the developed countries. It is estimated that more than 60% lung cancer patients receive radiation therapy, either for definitive treatment or for palliation, as part of their treatments. Intensity modulated radiation therapy (IMRT) has been known to produce highly desirable conformal dose distribution. The goal of IMRT in this setting is dose escalation to achieve more localized treatment with greater accuracy and thus, to improve tumor control and survival. However, it is very difficult to implement if there is a significant uncertainty in target delineation. Inaccurate target delineation could compromise the treatment outcome and may damage the normal lung tissue and other critical organs. This risk is particularly high in instances where the dose escalation or concurrent boost techniques are employed [1]. Therefore, it is imperative to have an imaging modality that provides an accurate diagnosis of lung cancer and thus, improves the accuracy of target volume delineation and minimizes the irradiated volume of organs at risk (OAR) for IMRT treatment planning.

Yulin Song is with the Department of Medical Physics, Memorial Sloan-Kettering Cancer Center, New York, NY 10021 USA (corresponding author, phone: 973-983-7311; fax: 973-983-7301; e-mail: songy@mskcc.org).

Maria Chan is with the Department of Medical Physics, Memorial Sloan-Kettering Cancer Center, New York, NY 10021 USA (e-mail: chanm@mskcc.org).

Chandra Burman is with the Department of Medical Physics, Memorial Sloan-Kettering Cancer Center, New York, NY 10021 USA (e-mail: burmanc@mskcc.org).

Donald Cann is with the Department of Radiation Oncology, Memorial Sloan-Kettering Cancer Center, New York, NY 10021 USA (e-mail: cannd@mskcc.org).

The rapid advancements in ^{18}F-labled fluorodeoxyglucose (^{18}FDG) positron emission tomography (^{18}FDG-PET) have made ^{18}FDG-PET a valuable non-invasive tool for the characterization and staging of lung cancer, detection of distant metastases and diagnosis of recurrent disease. Particularly, the hybrid PET/CT scanners have greatly improved the accuracy of the image co-registration. In addition, PET/CT also provides a more accurate attenuation correction map for standardized uptake value (SUV) quantification. Despite the distinct advantages of PET, there are still unsolved issues in treatment planing. These include variation in inter-modality and intra-observer delineated target volumes derived from PET/CT and CT, impact of different window and level settings of drawing monitors on target volume delineation, and uncertainty in auto-segmentation in target volume due to PET's low spatial resolution. In this study, we investigated the variation in inter-modality delineated target volume defined by two imaging modalities for lung cancer: CT and ^{18}FDG-PET/CT and its dosimetric implications in intensity modulated radiation therapy (IMRT).

II. MATERIALS and METHODS

A. CT and PET/CT Imaging

Treatment planning CT images were acquired using a GE LightSpeed CT scanner. Patients were scanned in a supine position in a customized thermoplastic mold to minimize patient movement during the procedure. Axial slices of 2.5 mm thickness and matrix size of 512 x 512 were acquired from the thoracic inlet to the costophrenic angles. CT images were transferred to our in-house treatment planning system in DICOM format for subsequent treatment planning.

Following the treatment planing CT imaging, PET/CT studies were then performed using a GE Discovery PET/CT scanner. The treatment planing position was reproduced in the PET/CT scanner by using the same immobilization device. Approximately one hour following the intravenous administration of ^{18}FDG (17.0 ~ 20.0 mCi), a whole-body PET scan was performed from the base of the skull to the mid thigh. As a part of the PET/CT imaging protocol, a CT scan of diagnostic quality was also acquired over the same region for the attenuation correction and treatment planning CT and PET/CT co-registration purposes. The emission data were reconstructed in the coronal, sagittal, and axial planes. The body weight adjusted standardized uptake values (SUV) were calculated for the regions of interest (ROI). PET/CT images were transferred to our in-house treatment planning

1-4244-0033-3/06/$20.00 ©2006 IEEE.

system for image co-registration and target volume delineation.

B. Image Co-registration and Target Delineation

All image co-registrations were accomplished using our in-house image co-registration software available within our treatment planning system. Treatment planning CT was first co-registered with the CT of PET/CT using a mutual information algorithm. Once this was completed, the co-registration between the treatment planning CT and PET was automatically generated. The main drawing window displayed the treatment planning CT image and the secondary drawing window displayed the corresponding PET image of the co-registered study (Figure 1). Volumes could be drawn on either of these windows and were saved to the treatment planning CT. For consistent target delineation on PET images, programmed window-level values were used, but they were allowed to be adjusted by the user.

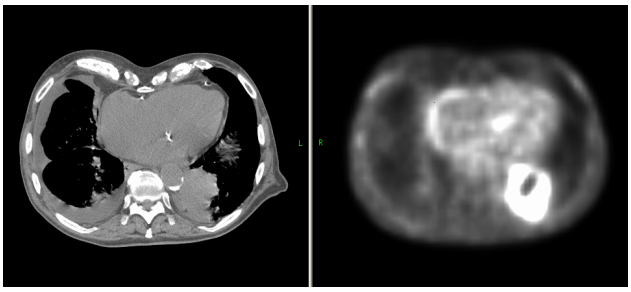

Figure 1. Demonstration of the volume delineation tool. The main drawing window on the left shows the treatment planning CT image, while the secondary drawing window on the right shows the corresponding PET image of the co-registered study. Volumes can be drawn on either window and are transferred to the opposite window automatically.

For this study, two gross tumor volumes (GTV), CT-GTV and PET-GTV, were delineated by the same radiation oncologist. The CT-GTV was delineated based on CT alone. A hardcopy of the diagnostic CT scan and the radiologist's diagnostic report were available to the radiation oncologist. The PET-GTV was defined based on PET alone. To make the volume delineation more objective, the CT-GTV and PET-GTV were delineated at different times. In both cases, the GTV consisted of the primary tumor and identifiable pathologically positive lymph nodes. Figure 2 shows the CT-GTV and the PET-GTV for patient No. 1 on a representative image slice.

C. IMRT Treatment Planning

For IMRT treatment planning, two planning target volumes (PTV) were created. The CT-PTV and PET-PTV were generated by adding a uniform 1.5 cm margin to the CT-GTV and PET-GTV, respectively. This was to account for target uncertainty caused by patient treatment setup error, breathing motion, and spontaneous organ movement. To achieve a better target dose coverage, an expanded PET-PTV, named as PET-PTVE, was also created by adding a uniform 3 mm margin to the PET-PTV. In addition, the planner also copied it above and below the PET-PTV by 2 slices to avoid cold spots in these regions. It should be pointed out that the PET-PTVE expanded into lung tissue regions was necessary to compensate for some of the effects of lateral disequilibrium that were observed in Monte Carlo dose calculations, but not accounted for with the standard dose calculation algorithms.

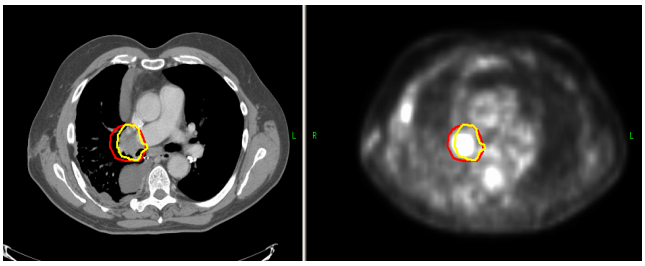

Figure 2. CT-GTV and PET-GTV shown on a representative image slice. The red solid line represents the PET-GTV and the yellow solid line represents the CT-GTV. The image on the left is the treatment planning CT and the image on the right is PET.

The organs at risk (OAR) were the cord and lungs, CORD and LUNGS, which were delineated by the treatment planner. To better spare the cord, a 3 mm uniform margin was added to CORD to create CORDE. Additionally, two tuning structures, INRIND and OUTRIND, were also created for "dose tuning" purpose. INRIND was created by adding a 6 mm uniform margin to the PET-PTVE. OUTRIND was generated by adding a 40 mm or more uniform margin to the PET-PTVE. By assigning proper dose constraints to INRIND and OUTRIND, they could be used to fine tune the dose outside the PET-PTV and thus, to eliminate the undesirable hot spots in these areas. Additional normal tissue structures could also be defined as needed. Figure 3 shows the volume definitions for a representative slice for patient No. 3.

Each IMRT plan consisted of five co-planner beams. The beam angles were approximately equally spaced between anterior-posterior (AP) and posterior-anterior (PA) directions. More beams would certainly produce a more conformal target dose distribution. However, they would also deliver unnecessary low dose to a larger lung volume. Efforts were made to avoid using the beams that passed through the cord. To spare the contra-lateral lung, the beams entered the target through the involved lung only. Optimization-only structures included PET-PTVE, CORDE, LUNGS, and RIND defined as the logical operation: OUTRIND-INRIND. The plan evaluation structures were PET-PTV, PET-GTV, CT-PTV, PET-GTV, CORD, and LUNGS.

Given a set of dose limits and dose-volume constraints to the optimization-only structures, the IMRT plans were optimized by minimizing a quadratic objective function

using an iterative gradient search algorithm. The objective function consists of terms corresponding to the targets and the organs at risk:

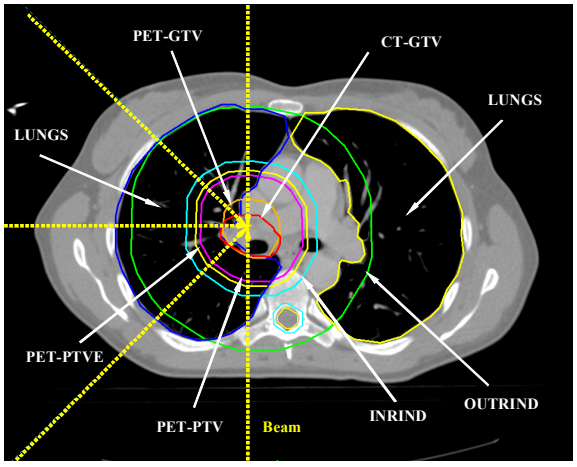

Figure 3. Structure definitions and beam angle selection. In this particular case, the tumor was in the right lung. Thus, all the beams entered the target from the right side of the thorax to maximize the protection of the left lung.

$$F = F_{target-1} + F_{target-2} + \cdots + F_{OAR-1} + F_{OAR-2} + \cdots \quad (1)$$

The term for the target is given by:

$$F_{\text{target}} = \frac{1}{N_t}\left[\begin{array}{l} \sum_{i=1}^{N_t}(D_i - D_{presc})^2 \\ +w_{t,\min}\cdot\sum_{i=1}^{N_t}(D_i - D_{\min})^2\cdot\Theta(D_{\min} - D_i) \\ +w_{t,\max}\cdot\sum_{i=1}^{N_t}(D_i - D_{\max})^2\cdot\Theta(D_i - D_{\max}) \end{array}\right] \quad (2)$$

where N_t is the number of dose calculation points in the target, D_i is the dose to point i, and D_{presc} is the prescription dose. The second and third terms inside the brackets implement the target homogeneity criterion: D_{min} and D_{max} are the minimum and maximum tolerance doses, and $w_{t,min}$ and $w_{t,max}$ are the penalties or weighting factors associated with under- and over-dosing. $\Theta(x)$ is the Heaviside function, defined as:

$$\Theta(x) = \begin{cases} 1 & x \geq 0 \\ 0 & x < 0 \end{cases} \quad (3)$$

Similarly, the term for the organs at risk (OAR) is given by:

$$F_{OAR} = \frac{1}{N_{OAR}}\left[\begin{array}{l} w_{OAR,\max}\cdot\sum_{i=1}^{N_{OAR}}(D_i - D_{\max})^2\cdot\Theta(D_i - D_{\max}) \\ +w_{OAR,dv}\cdot\sum_{i=1}^{N_{dv}}(D_i - D_{dv})^2\cdot\Theta(D_i - D_{dv}) \end{array}\right] \quad (3)$$

where the first term inside the brackets implements a maximum dose constraint D_{max} on the OAR and the second a dose-volume constraint. The relative penalty weights are given by $w_{OAR,max}$ and $w_{OAR,dv}$ respectively. N_{OAR} is the number of points in the OAR and N_{dv} the number of points whose dose must be below the dose-volume constraint dose D_{dv}.

The dose to point i, D_i, is the sum of dose contributions from all rays:

$$D_i = \sum_{j=1}^{N_r} x_j a_{ij} \quad (4)$$

where N_r is the number of rays, x_j is the intensity of the j-th ray, a_{ij} the dose deposited to the i-th point per unit intensity of the j-th ray, and the product is summed over all j.

The goal of IMRT optimization was to find the set of ray intensities x_j that minimized the objective function given by Equation (1). If the criteria for plan acceptance were not met, a trade-off between the target dose coverage and constraints would have to be made. Once optimal intensity maps were obtained, leaf sequences were generated using the dynamic MLC (DMLC) technique. Based on these leaf sequences, the final dose distribution was then computed using a pencil beam algorithm.

III. RESULTS

A. GTV, PTV, and PTVE Analysis

Five patients from a total of ten patients who have recently received ^{18}FDG-PET/CT imaging studies in our regional center were randomly selected for this study. Three of the patients had right lung cancer and two had left lung cancer. Comparison of CT-GTV, PET-GTV, CT-PTV, and PET-PTV, CT-PTVE, and PET-PTVE is shown in Table 1 for three of the patients.

Table I.
Comparison of CT-GTV, PET-GTV, CT-PTV, PET-PTV, CT-PTVE, and PET-PTVE (cm^3)

	Patient No.1	Patient No.2	Patient No.3	Mean
CT-GTV	43.25	233.40	15.24	97.30
PET-GTV	73.61	308.05	28.37	136.68
CT-PTV	138.31	573.92	60.27	257.50
PET-PTV	197.61	673.32	101.15	324.03
CT-PTVE	165.47	661.68	68.94	298.70
PET-PTVE	253.11	788.59	135.42	392.37

As indicated in Table 1, the PET-defined GTV, PET-GTV, was consistently larger than the CT-defined GTV, CT-GTV, for all three cases. The differences between PET-GTV and CT-GTV were 30.26, 74.65, and 13.13 cm^3 for patient No. 1, No. 2, and No. 3, respectively. In terms of percentage, the differences were 70.2, 31.98, and 86.15%, respectively. It is interesting to note that the smaller the CT-GTV, the larger the percentage difference in the PET-GTV. The differences between PET-PTV and CT-PTV were 59.30, 99.40, and 40.88 cm^3 for patient No. 1, No. 2, and No. 3, respectively. The percentage differences were 42.87, 17.32, and 67.83%, respectively. As expected, the volume differences between PET-PTVE and CT-PTVE were even bigger, being 87.64, 126.91, and 66.48 cm^3, respectively. The volume difference between PTVE and PTV is approximately linearly proportional to $\sim(R_{PTVE}^3 - R_{PTV}^3)$, where R_{PTVE} is the mean radius of PTVE and R_{PTV} the mean radius of PTV. The percentage differences were 52.96, 19.92, and 96.43%, respectively.

B. Target and OAR Dose Analysis

The prescription dose for all five cases was 64.8 Gy. Table 2 shows the dose statistics for CT-GTV, CT-PTV, PET-GTV, PET-PTV, CORD, and LUNGS. The values shown are in percentage, i.e., normalized to the prescription dose. As shown in Table II, the dose statistics for CT-defined volumes were very similar to those for PET-defined volumes for patient No. 1. This essentially reflects the fact that CT-GTV and PET-GTV were approximately concentric. There was also no significant shift between the two. In addition, each image slice contained both CT-GTV and PET-GTV. In contrast, there was a big difference in minimum dose D_{min} between CT-GTV and PET-GTV for patient No. 2. This was due to the fact that there was a big shift between CT-GTV and PET-GTV in the superior-inferior direction. In addition, we also computed the normal tissue complication probability (NTCP) and fractional lung units damaged (f_{dam}). Figure 4 shows the dose distribution of a representative slice for patient No. 3.

Table II.
Dose Statistics for CT-GTV, PET-GTV, CT-PTV, PET-PTV, OARs (%)

Patient No. 1	D_{max}	D_{min}	D_{mean}	D_{95}	V_{95}	NTCP	f_{dam}
CT-GTV	102.08	96.66	99.36	97.86	100.0	NA	NA
PET-GTV	102.71	94.65	99.42	97.58	99.98	NA	NA
CT-PTV	102.79	94.44	99.32	97.14	99.90	NA	NA
PET-PTV	102.52	93.75	99.22	96.87	99.84	NA	NA
CORD	39.79	0.25	7.11	0.29	0.0	NA	NA
LUNGS	101.92	0.08	20.10	0.39	5.74	0.0	0.0

Patient No. 2	D_{max}	D_{min}	D_{mean}	D_{95}	V_{95}	NTCP	f_{dam}
CT-GTV	115.66	12.63	103.37	96.56	97.46	NA	NA
PET-GTV	116.49	92.67	104.24	99.19	99.74	NA	NA
CT-PTV	116.63	13.07	101.65	87.13	92.96	NA	NA
PET-PTV	116.27	50.39	103.51	97.83	97.58	NA	NA
CORD	60.29	2.25	27.71	3.01	0.0	NA	NA
LUNGS	108.97	0.17	18.52	0.63	5.36	0.0	0.0

Patient No. 3	D_{max}	D_{min}	D_{mean}	D_{95}	V_{95}	NTCP	f_{dam}
CT-GTV	107.21	101.40	104.72	102.95	100.00	NA	NA
PET-GTV	107.04	100.32	104.36	102.51	100.00	NA	NA
CT-PTV	107.12	97.61	104.35	101.98	100.00	NA	NA
PET-PTV	106.96	99.93	104.12	101.70	100.00	NA	NA
CORD	41.71	0.11	8.60	0.16	0.0	NA	NA
LUNGS	106.68	0.03	17.41	0.33	4.04	0.0	0.0

Abbreviations: D_{max}: maximal dose; D_{min}: minimal dose; D_{mean}: mean dose; D_{95}: dose covering 95% volume; V_{95}: volume receiving 95% prescribed dose,

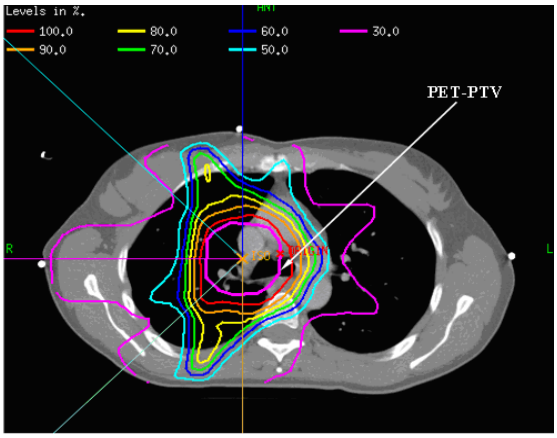

Figure 4. Isodose distribution of a representative slice for patient No. 3. The PET-PTV was very well covered in this example.

IV. CONCLUSIONS

Our preliminary data indicated that there was a big inter-modality variation in gross tumor volume defined by CT and ^{18}FDG-PET for lung cancer. ^{18}FDG-PET-defined GTVs were consistently larger than those defined by CT because ^{18}FDG-PET can better identify pathologically positive lymph nodes. The dosimetric effects could be significant if there was a volume shift between CT-GTV and PET-GTV in any direction, particularly in superior-inferior direction. If CT-GTV and PET-GTV were concentric, there would be virtually no dosimetric effects on the quality of an IMRT plan. Correct window/level setting was crucial for target volume delineation using ^{18}FDG-PET

REFERECE

[1] M.F. Chan, C.S. Chui, Y. Song, C. Burman, E Yorke, C. Della-Biancia, K. Rosenzweig, and K. Schupak, "Combination of electron and photon intensity modulated radiotherapy: A novel radiation therapy technique for the management of malignant pleural mesothelioma", *Radiother. and Oncol.* **79**(2):218-23, May 2006.